Polymer Testing 93 (2021) 106894

Contents lists available at ScienceDirect

Polymer Testing

journal homepage: http://www.elsevier.com/locate/polytest

Mechanical behaviour of double side high performance PSA adhesive applied to painted naval structures

M. Ortega-Iguña [a], M. Chludzinski [a], C. Churiaque [a], R.E. Dos Santos [a], M. Porrúa-Lara [b], F. Abad-Fraga [b], J.M. Sánchez-Amaya [a,*]

[a] Department of Materials Science and Metallurgical Engineering and Inorganic Chemistry, School of Engineering, University of Cádiz. Avenida de La Universidad de Cádiz, 10, E-11519, Puerto Real, Cadiz, Spain
[b] Navantia S.A., S.M.E., Bahía de Cádiz Shipyard, Industrial Estate S / N, E-11519, Puerto Real, Cadiz, Spain

ARTICLE INFO

Keywords:
Pressure sensitive adhesive (PSA)
Adhesion
Painted naval steel
Shear adhesion
Tensile adhesion
Toughness
Ductility

ABSTRACT

The use of adhesives constitutes a well-established technology in the aeronautical and automotive industries. A rising interest in the use of these materials has appeared in naval industry, where using adhesives in non-structural areas implies the reduction of welding to fix low weight components, making the joining process cheaper and faster. Among the different families of available adhesives, double-sided Pressure Sensitive Adhesives (PSAs) are considered of great industrial interest. A high performance PSA has been employed to join specimens of carbon steel coated with an epoxy painting scheme approved by the naval sector. The present paper reports for the first time the influence of some experimental application variables of this PSA-coated naval steel system on its mechanical behaviour. Standard shear and tensile tests have shown that the curing conditions, surface preparation and paint roughness have considerable effects on the resistance of these adhesive joints.

1. Introduction

Industrial development has led to the increasingly widespread use of modern, lightweight materials. In this context, there is an increasing demand for adhesives as bonding materials, since they are a light and cheap industrial solution [1–4]. In addition, they are easy to apply, and provide zero risk to the applicator [5]. Adhesive bonding is a well-established technology in the aeronautical and automotive industries, due to its low cost, good damping behaviour and mechanical properties [1,6–9]. It has been detected that there is a growing interest in the use of these materials in other industrial sectors, such as shipbuilding. This industry is exploring the possibility of using adhesives in non-structural areas of the ship that are generally welded, such as component supports or lightweight parts. This change would speed up the bonding process and make it cheaper [1–3,6,7].

Adhesives are especially interesting in shipbuilding to joint non-structural components to already painted (and sometimes already certified) structures, as bulkheads and decks (common naval terms to refer to ship walls and ceilings, respectively). These components can be fixed to bulkheads at both vertical and horizontal positions, the adhesives mainly working at shear stress. The components can also be joined to deck ceilings at overhead position, the adhesive mainly working in this case at tensile stress. The main advantages of using adhesives, in comparison with traditional welding techniques, rely on the low price and easy application. Thus, if a component is required to be joint by welding to painted structures, the process needs to sandblast the joining surfaces before welding, and re-paint the zone after welding. Sometimes, the painted structures have been certified by the customer before detecting the need of joining the components. In this cases, welded and re-painted structures need to be again certified, making this traditional welding process a very expensive and time consuming joining technology. From this point of view, the use of adhesives is clearly advantageous to joint pieces to painted surfaces, as there is no need to sandblast and repaint the structure, as they can be directly applied to coated zones. Re-certification processes are also avoided with adhesives.

Recently, many industrial sectors have opted for the use of adhesive tapes. These adhesives are attracting interest as they do not require post-application treatments [1]. There are different types of adhesive tapes, mainly classified into two groups: single-sided adhesive films and double-sided adhesive tapes. The former one generally consists of a rigid film of adhesive, usually employed for sealing, retention and repairing works. On the other hand, double-sided adhesive tapes, including

* Corresponding author.
E-mail address: josemaria.sanchez@uca.es (J.M. Sánchez-Amaya).

https://doi.org/10.1016/j.polymertesting.2020.106894
Received 9 July 2020; Received in revised form 8 September 2020; Accepted 10 October 2020
Available online 13 October 2020

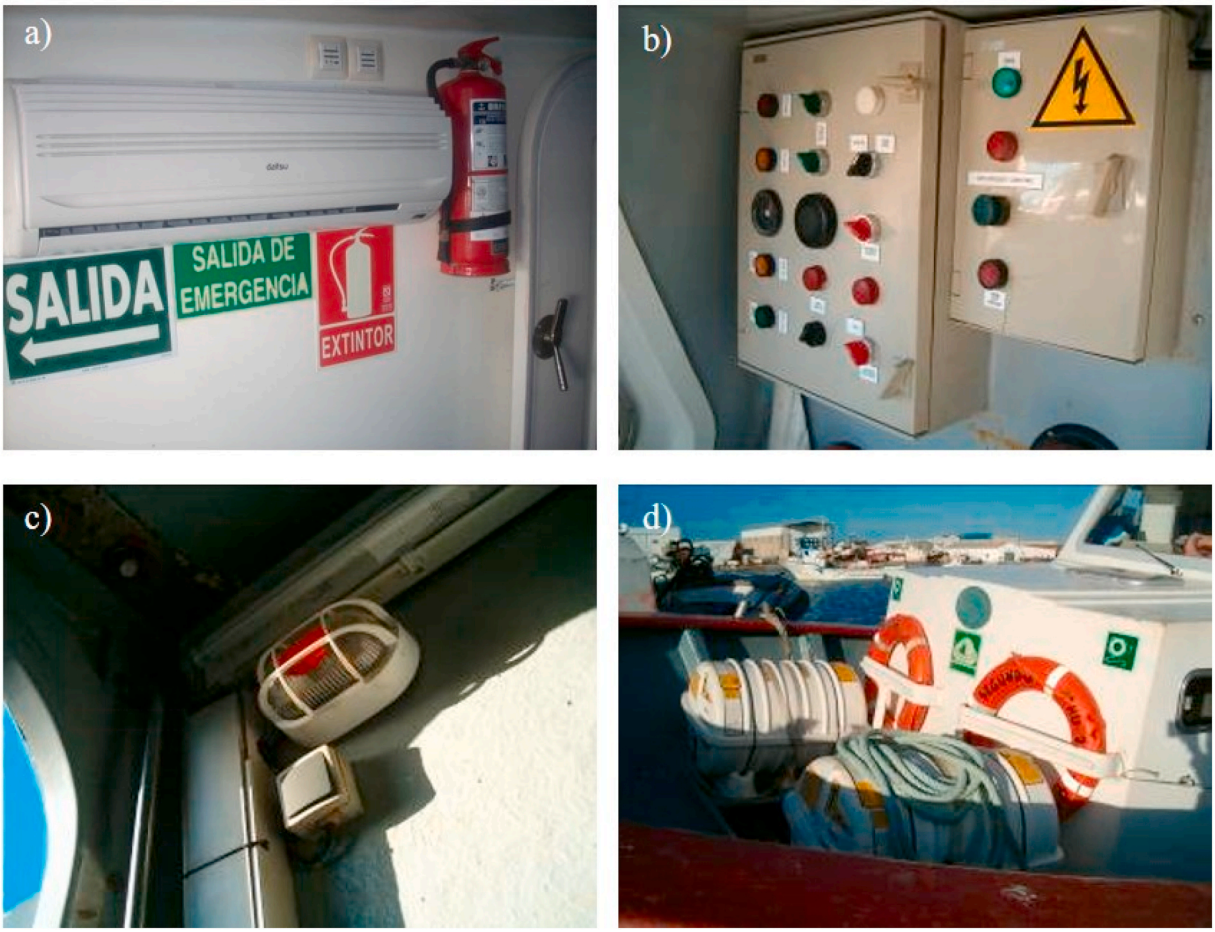

Fig. 1. Examples of components which can be fixed by PSA to bulkheads: a) split air conditioner, b) electrical panels, c) lights and switches and d) signage.

Pressure Sensitive Adhesives (PSAs), are generally used to bond substrates. PSAs generally consist of a flexible viscoelastic backing, with a layer of adhesive at both parts of this backing that generates the joint by contact under pressure [1]. Currently, PSAs are actively applied in different industrial sectors, such as aerospace and the automotive sector [6].

Currently, there is a wide variety of PSAs that differ in the nature of the adhesive base (acrylic, rubber or silicone), the supporting material (backing), and the manufacture process. Most PSAs used at the industrial level are acrylic, due to the diversity of acrylic monomers and their good properties. The most important properties for the industrial sector are: low price, self-adhesive properties, and the high resistance to weathering [7]. To achieve these properties, different polymers are mixed, adjusting their molecular weight and distribution. This is carried out by copolymerization reaction with a polar monomer and by varying the curing system [10–13]. Acrylic PSAs are usually made up of three main segments [6]: i) Soft monomers with a low glass transition temperature (Tg), necessary to give the material stickiness; ii) Hard monomers with a high Tg, which provides internal strength to the adhesive; and iii) Functional monomers, such as acrylic acid, in order to provide active centres to the adhesive.

Within the high range of available PSAs, a relatively new generation of these adhesives are available in the market, catalogued as of high performance. These high performance PSAs differ from the common

Fig. 2. Examples of components which can be fixed by PSA to ceiling in overhead position: a) naval lights, c) cable trays.

Table 1
Chemical composition of naval carbon steel S355 J2 + N (wt. %).

Chemical Composition (wt. %)	C	Si	Mn	P	S
	≤0.20	≤0.03	≤1.60	≤0.04	≤0.04

acrylic PSAs in the internal structure of the polymer, which is modified by adding different monomers during the adhesive polymerization reaction and by diffusion of enhancers [14]. These monomers give the adhesive a greater elastic modulus and resistance to temperature, to solvents and to gas permeability [1,15–17].

PSAs are nowadays used to bond a large number of surfaces, as polymethacrylate [2], stainless steel and polyisobutylene [18], polypropylene [19], glass [20], and aluminium and carbon fiber reinforced polymer (CFRP) [21]. Depending on the characteristics of the surfaces to be joined, paying special attention to surface energy, the behaviour of these PSAs can be modified by different surface treatments. These surface treatments work by introducing active functional groups that lead to better wettability and adhesion for low surface energy surfaces [22–25]. Another factor to take into account to achieve good mechanical contact between the surfaces to be joined is the surface roughness. According to Ref. [26], a high average roughness of the adhesive or substrate may cause incomplete bonding, due to the presence of air bubbles trapped at the interface between the adhesive and the surface. These bubbles can act as nucleation sites for cavities in the early stages of the failure process [26]. On the other hand, the performance of the PSA has been reported to be affected by the degree of polymer crosslinking [9]. The thickness of the tape determines the flexibility properties of the adhesive, and with it, its possible applications [27], while the degree of polymer crosslinking defines the PSA adhesion ability [8,12].

The use of different types of adhesives in the shipbuilding industry is being increased [28]. However, according to the research literature revised, as far as the authors are concerned, PSAs have not been yet used to join substrates coated with paints approved by the naval sector. The use of this type of adhesives could be an excellent alternative to the welding process of non-structural elements. Figs. 1 and 2 depict different examples of components usually connected to coated steel in shipbuilding industry, and therefore, possible candidates to be joint by PSA. Fig. 1 shows examples of components joined to bulkheads, while Fig. 2, to overhead sealings. As stated above, the replacement of welding of not critical components by PSAs would imply a lower cost of the joining process, as well as a saving in manufacturing time.

As stated previously, no published research studies dealing with the use of PSAs to join coated naval steel elements have been reported. In fact, very little is known so far about the application possibilities of this bonding technology to substrates coated by painting schemes approved by the naval sector. The present paper aims to cover this gap of technological and research knowledge. The concise objective of this contribution has been focussed on studying the mechanical behaviour (including both shear and tensile resistance) of a high performance PSA to join steel samples coated with a naval painting scheme. The effect of different experimental parameters related to the application conditions of this PSA has been analysed. Thus, the influence of the surface roughness, surface preparation, curing time, compression force and compression time is deeply analysed. The mechanical strength of the joints is tested by standard tensile tests to simulate the bonding behaviour of the component to the painted structure of the ship. Shear tests are carried out to simulate the joints of components to painted bulkhead, while tensile tests are performed to evaluate the behaviour of PSA when used to join elements at the painted ceiling of the ship.

2. Materials and methods

Samples of naval carbon steel S355 J2 + N (UNE-EN ISO 10025), whose composition is detailed in Table 1, were sandblasted to Sa 2 ½ grade. These samples were covered

with an epoxy paint scheme commonly used by the naval sector. The scheme is made of 3 layers, two 300 μm thick internal layers of PPG Sigmashield 880 (two epoxy components cured with a high thickness polyamine adduct, Sigma Coatings, PPG Protective and Marine Coatings, Pittsburgh, Pennsylvania, U.S.) and one 125 μm thick external layer of PPG PSX700 (two siloxane based components, PPG PSX700, PPG Protective and Marine Coatings, Pittsburgh, Pennsylvania, U.S.).

Fig. 3 presents the schemes of the 3 experimental assemblies mounted to perform the mechanical tests. Fig. 3a shows the assembly used to perform the shear mechanical tests, while Fig. 3b and c depict the mounted assemblies employed to carry out the tensile tests.

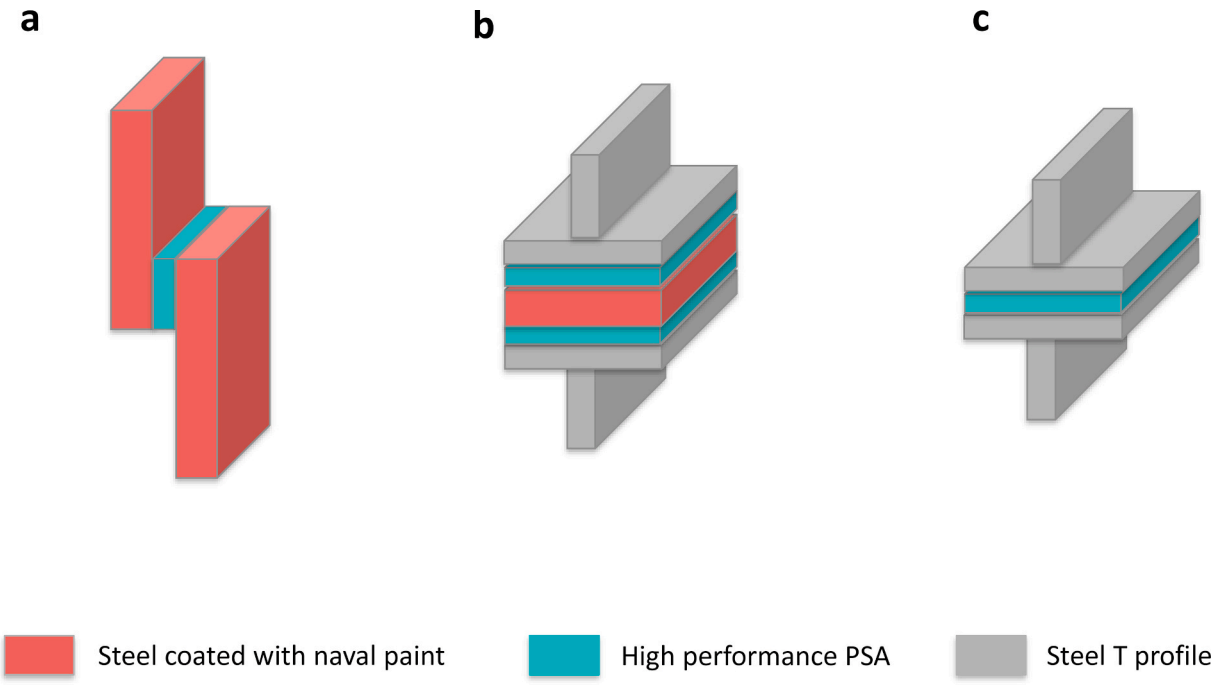

Fig. 3. Joint assemblies to perform: (a) shear tests to painted samples, (b) tensile tests to painted samples, and (c) tensile tests to bare samples.

Table 2
Surface Treatments applied to samples before joining to PSA.

Method identification	Surface Treatment
T_1	Cleaning with dry paper
T_2	Cleaning with isopropanol
T_3	Cleaning with isopropanol + application of adhesion promoter (FCP 60153)

Table 3
Parameters values of analysed curing conditions (reference parameters recommended by the manufacturer highlighted in bold).

Parameter	Unit	Parameter Values				
Compression force	Newton (N/cm^2)	10	**15**	30		60
Compression time	Minutes (min)	0.5	**1**	5		10
Curing time	Hours (h)	0	6	24	**72**	168

Before mounting the assemblies shown in Fig. 3, the surface roughness of the different samples was measured using a roughness meter adapted with a surface probe (Perthmeter PGK 120, Mahr), placing the measuring probe on the surfaces so that it ran through the area to be joined. The roughness values reported in the paper correspond to the mean arithmetic roughness parameter (R_a). Note that two different surfaces were considered, the external paint layer of the coated naval steel samples, and the surface of the bare steel T-profiles used in assemblies shown in Fig. 3b and c. Note that these T surfaces were ground with 1200 grit water grinding paper before the roughness measuring.

After roughness measurements, the samples were subjected to different cleaning procedures, all of them proven experimentally to keep the paints unaltered, that is, assuring that the products used do not dissolve the external layer of the painting scheme. In order to evaluate the influence of the cleaning methodology on the mechanical resistance of the joints, three different surface treatments were tested, encoded as T_1 to T_3, as summarised in Table 2. T_1 was based on a simple process consisting of a careful removal of dust with standard commercial dry laboratory paper. T_2 consisted of a cleaning with paper impregnated with isopropanol. In T_3 procedure, samples were firstly cleaned with

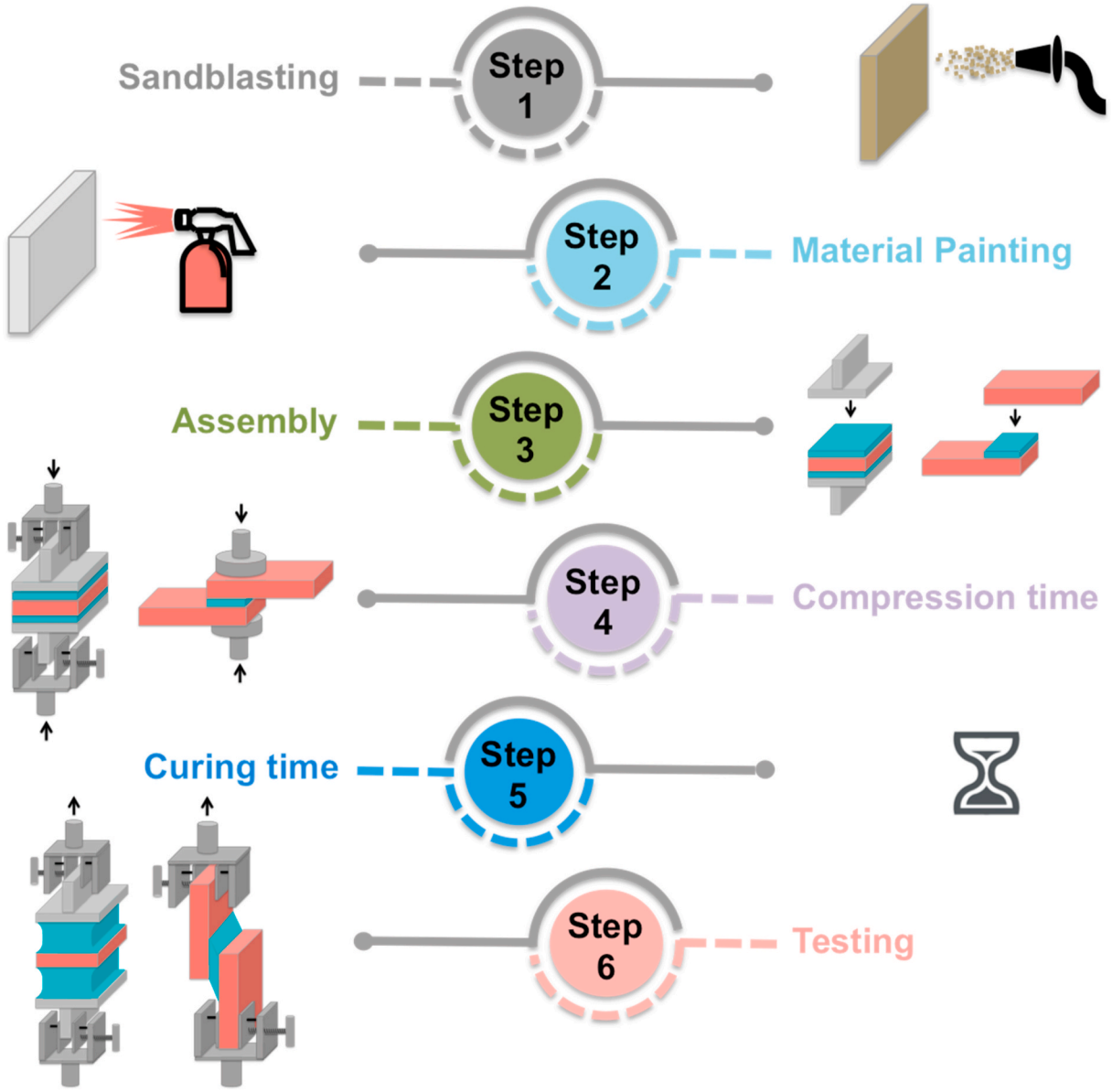

Fig. 4. Scheme of the overall experimental procedure followed to prepare and test the PSA joints.

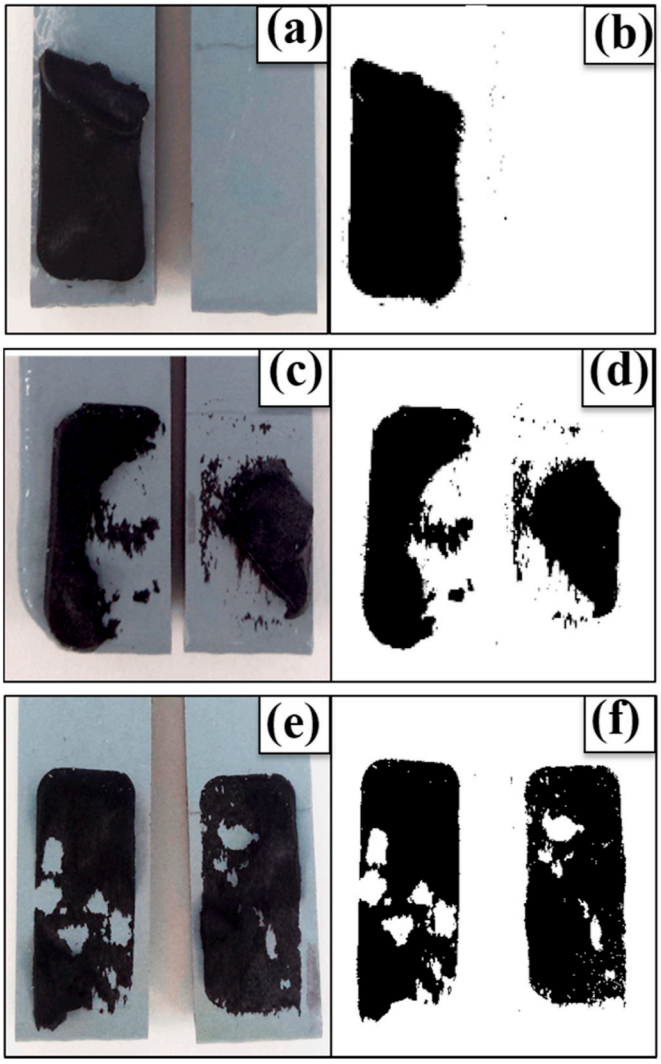

Fig. 5. Examples of real images (*a, c* and *e*) and software treated images (*b, d* and *f*) of samples after shear tests with surface treatment T_1 (images *a* and *b*), T_2 (images *c* and *d*) and T_3 (images *e* and *f*).

paper impregnated with isopropanol and subsequently treated with an adhesion promoter (FCP 60153, TESA).

After cleaning the samples, the different joints were assembled, as described in Fig. 3. A high performance PSA (double-sided adhesive tape composed of polymer foam, reference 92,111, TESA, Germany) was used for all joints. This PSA is commercially catalogued as high initial bonding performance, claimed to provide superior bonding performance right after application. This PSA is a double-side black foam with a thickness of 1.1 mm. It is distributed in different formats; rectangular sections of 1.0 × 1.9 cm^2 of area were used in this study.

The application of PSA involves the control of different experimental parameters. The curing process is fundamentally conditioned by three parameters: the curing time, the compression force and the compression time. In order to achieve the maximum mechanical performance of the PSA used in the present work, these three aforementioned variables were studied. After cleaning the samples, the joints were assembled and subjected to a compression process, with controlled values of time and pressure, using a Shimadzu universal test equipment with a capacity of 10 kN. Once the joint was compressed, it was allowed to cure for a period of time and subsequently tested. The different joint probes were obtained by modifying the values of one of the different curing variables described, leaving the remaining parameters fixed. These values are specified in Table 3.

After the compression step, the assembly joints were left to cure at room temperature (21 °C) and a relative humidity of 60%. After the curing time, the joints were subjected to mechanical tensile tests. The lap assembly joints shown in Fig. 3a allowed the evaluation of the shear resistance of joints, while the tensile resistance were tested by the joints shown in Fig. 3b and c. Both shear and tensile tests were carried out at a constant speed of 10 mm/min, following the recommendations of the Standard ISO 15870. All mechanical tests have been performed in triplicate in order to check the reproducibility, and to estimate the average and standard deviation of results. Different mechanical properties have been extracted from the obtained Stress-Strain curves: Ultimate Tensile Strength, UTS (the maximum stress values provided by the Stress-Strain curve), Ductility (Elongation at fracture), and static Toughness (overall area below the Stress-Strain curve, estimated by integration of the 6th degree full polynomial that better fitted to each curve).

Fig. 4 summarised the overall experimental procedure followed, including all the steps described above, as sandblasting, painting, PSA assembly preparations, compression, curing, and testing.

After testing the joints, the evaluation of the rupture model was performed according to the criteria established in the UNE-ISO 10365 Standard. To precisely define the type of fracture, image analysis software was used to calculate the proportion of the total area of adhesive remaining on each side of the joint. This result is an index, a percentage of cohesive failure of the bond. The best possible output is to have a 100% of cohesive rupture, indicating that the whole area of PSA has properly adhered to the substrate and, therefore, that it works effectively opposing resistance to the efforts. Meanwhile, low percentage of cohesive failure means that low effective adhesion between the PSA and coated samples takes place, resulting in an adhesive rupture.

Fig. 5 shows examples of real images and software treated images to estimate the percentage of cohesive failure. Images *a, c* and *e* are real images, obtained with a camera, while *b. d* and *f* are those obtained after software analysis treatment of real images. In the examples of the figure, a sample subjected to cleaning procedure T_3, images e and *f*, underwent a cohesive rupture close to 100%. The opposite took place for a sample after T_1, corresponding to images *a* and *b*, where a 100% of adhesive failure is observed. Images *c* and *d*, obtained after T_2, show an intermediate behaviour, reflected in a 65% of adhesive failure.

3. Results and discussion

3.1. Comparison between PSA adhesion to bare steel and to painted steel

In this first section of the results, the adhesion provided by the high-performance PSA when joining bare steel samples is compared to that obtained when joining painted samples. Before performing the mechanical tests, the roughness of both kinds of surfaces was measured. Fig. 6 shows the roughness, in terms of R_a values, of painted samples and bare surfaces used in the present study. It can be observed that the roughness of the paint is almost the double than that of bare steel.

Joint assemblies were prepared following the schemes shown in Fig. 3 (b and c), using bare T steel supports. Reference curing conditions were followed in these tests: Compression force of 15 N, Compression time of 1 min, and Curing time of 72 h. Surface treatment T_3 was applied to the samples. After completing the bonding process, 3 replicas of each system were subjected to tensile tests. The average and standard deviation of the obtained maximum tensile strength (UTS) values are presented in Fig. 7. Slightly higher UTS values were measured for the bare steel. These results bring to light the good performance of the optimized curing conditions applied to PSA. The UTS values of the PSA 92111 were slightly higher than those obtained by similar PSAs [29,30]. Interestingly, the strength of this high performance PSA is considerably higher than other standard commercial PSAs. Thus, after the optimization of the curing process, the PSA 92111 reached a UTS of 1.6 MPa, while the typical PSAs display values between 0.3 and 1 MPa [31–35].

Figs. 6 and 7 show that surface roughness is an important parameter

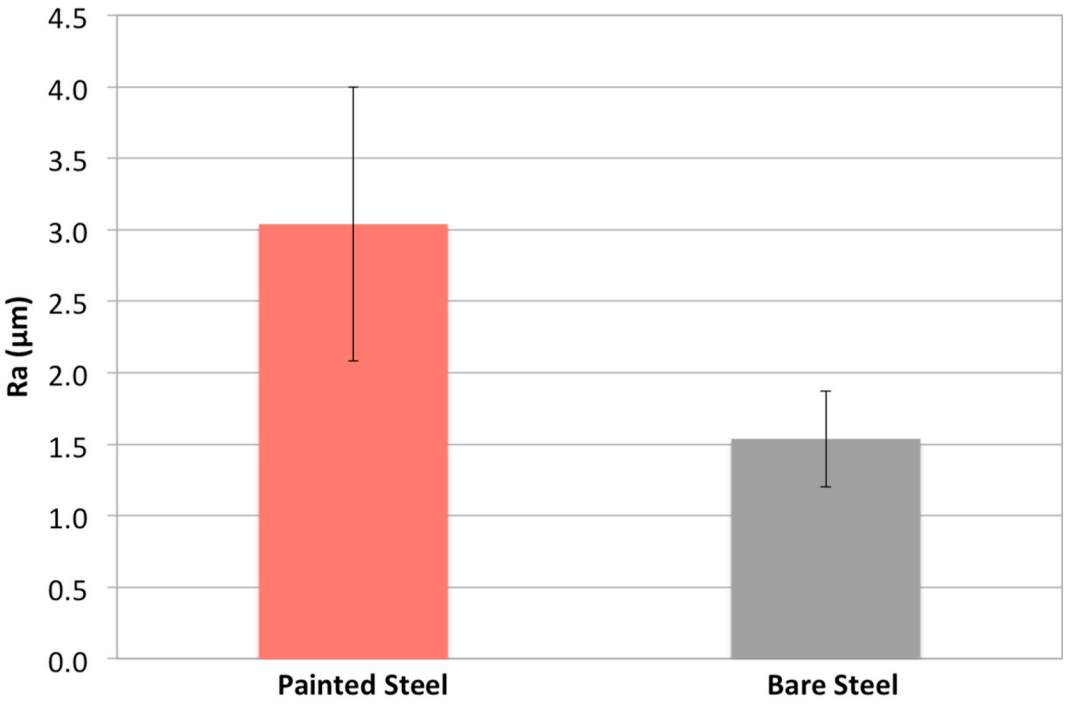

Fig. 6. Comparison between roughness (R_a) of painted and bare steel samples.

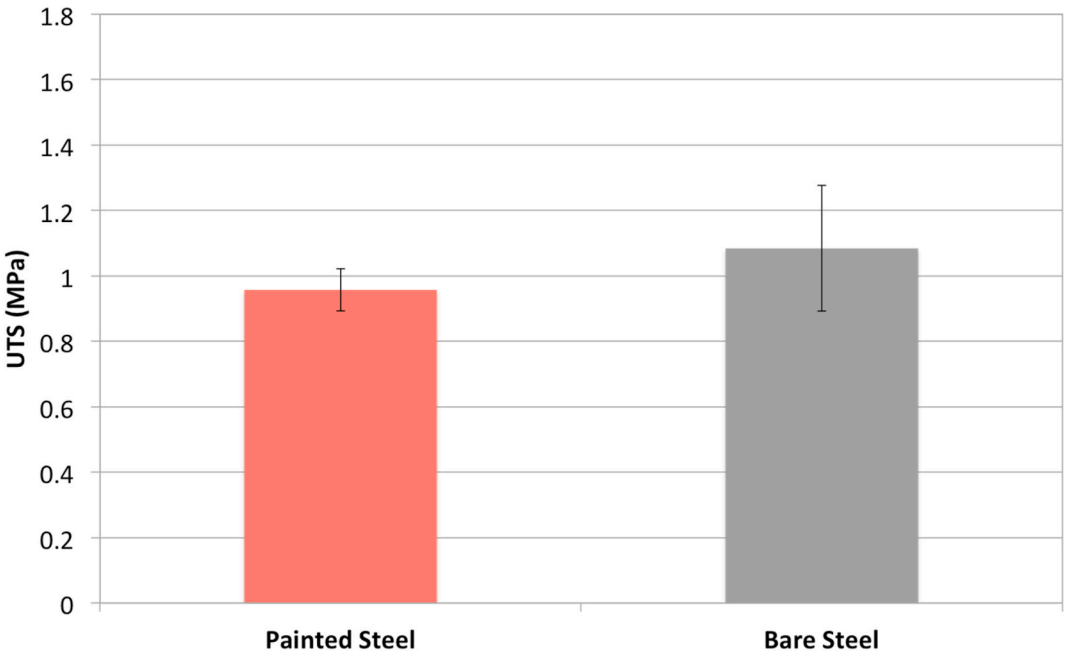

Fig. 7. Strength of the joint formed by steel surfaces joined with PSA and steel surface attached to painted surface.

in the adhesion process, and therefore decisive in the behaviour of the surface-PSA bond [27]. The slightly lower UTS values measured for the painted steel joint with respect to the bare steel are reported in previous works that can have its origin in a greater amount of air bubbles that can be trapped at the interface, due to their greater roughness, preventing a full contact painted steel-PSA [28]. In the present study, the authors relate this UTS decrease to the low surface energy of painted steel. Low surface energy is reported to limit the strength of the joint [28,37]. In fact, different surface treatments are studied in subsequent sections of this paper to achieve an increase in the surface energy of the painted steel and with it, strengthen the van der Waals bonds (dominant bonding of the PSA union), as well as accommodate the pH of the surface, improving the joint properties [38].

It is important to highlight the need to carry out the study reported in this section, to verify that the joint outlined in Fig. 3 (b) specifically evaluates the tensile strength of the painted steel-PSA joint. Fig. 7 shows that the bare steel-PSA connection is stronger than the painted steel-PSA connection. In fact, all tensile tests performed with scheme b of Fig. 3 in the present research were observed to fracture at the painted steel-PSA interface. With this, the proposed methodology for evaluating the tensile strength of painted steel-PSA by following this scheme b of Fig. 3 is validated and approved, as the PSA-bare steel connection is always

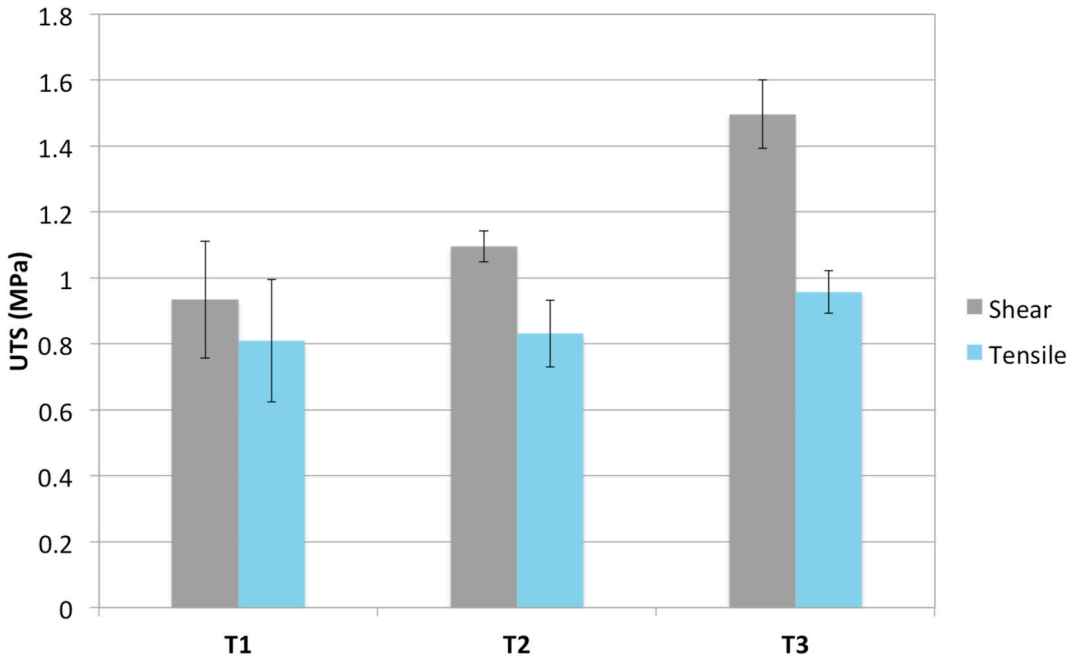

Fig. 8. Study of different surface preparation methods to improve the strength of the joint.

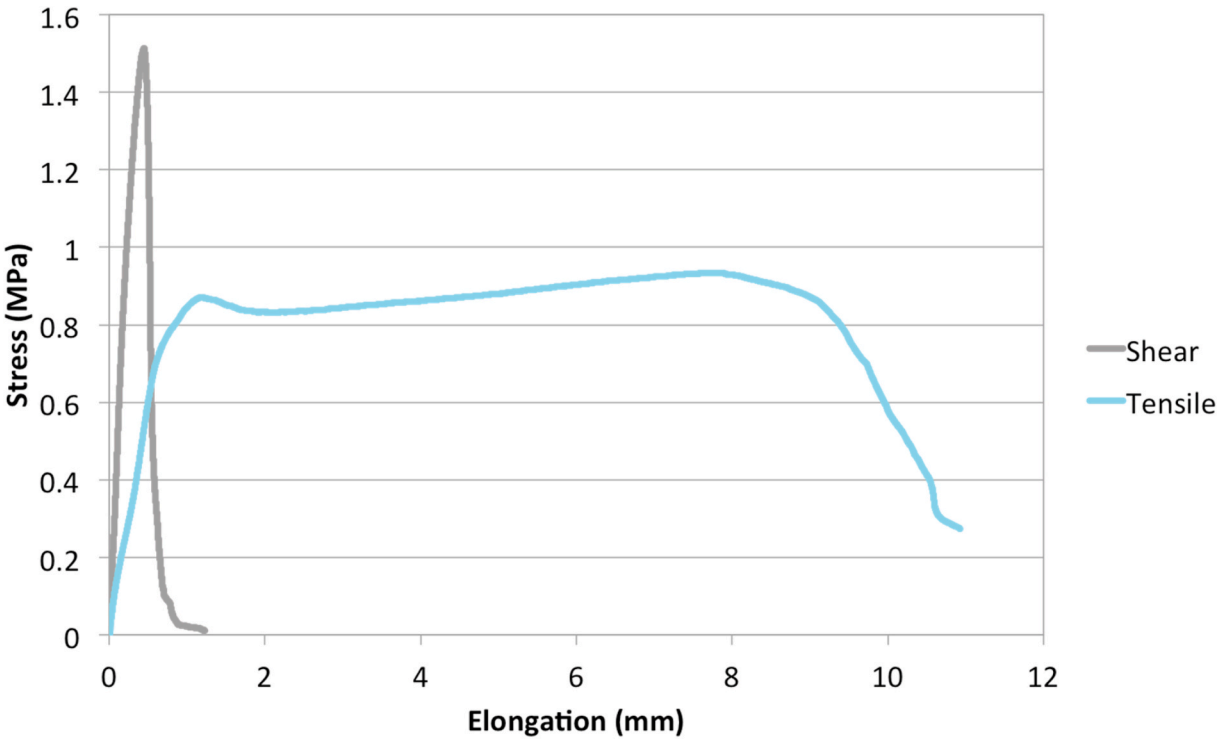

Fig. 9. Representative Stress-Elongation curves of tensile and shear tests of PSA joints.

stronger than the PSA-paint connection.

3.2. *Influence of surface treatment*

To counteract the effect of the low surface energy of painted steel, the influence of surface preparation on the mechanical behaviour of joints has been analysed. For this, three different conditions have been evaluated (as indicated in Table 1): T_1 (paper cleaning), T_2 (isopropanol cleaning), and T_3 (isopropanol cleaning followed by adhesion promoter). The tests have been carried out maintaining the curing variables recommended by the manufacturer (highlighted in bold in Table 1). Fig. 8 shows the UTS results for shear and tensile configurations, assembled as shown in schemes a and b of Fig. 3, respectively. It can be seen in Fig. 8 that the adhesion in both configurations improves after applying the adhesion promoter (T_3). The fact of incorporating functional groups to a practically inactive surface, due to its low surface energy, implies an increase in wettability, and with it, an improvement in bond strength [23].

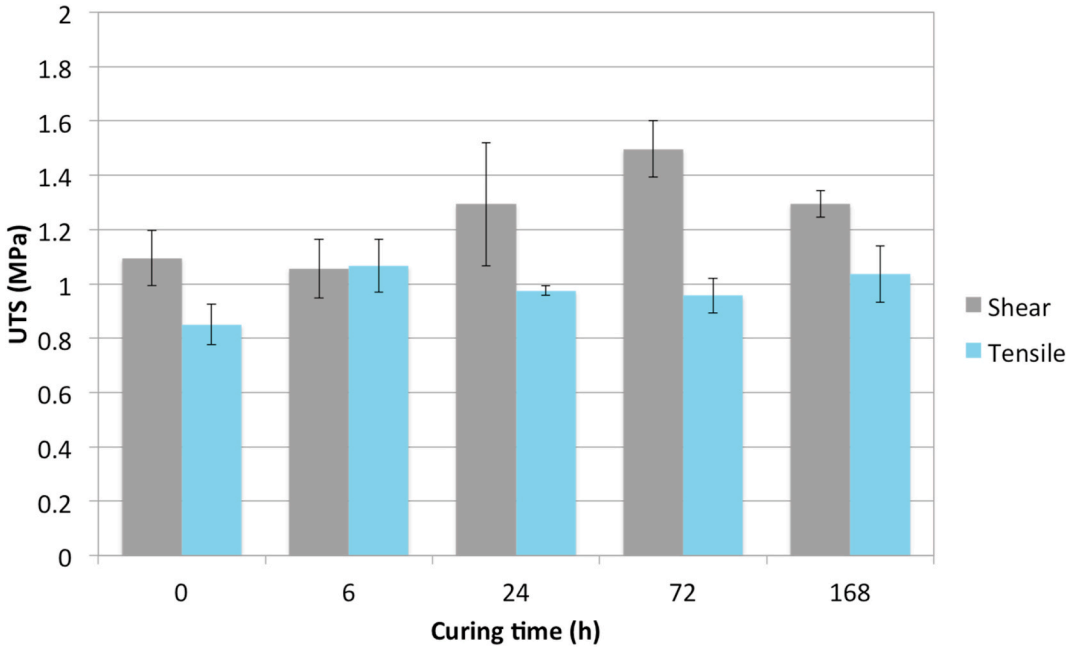

Fig. 10. Influence of PSA curing time on UTS values of shear and tensile tests.

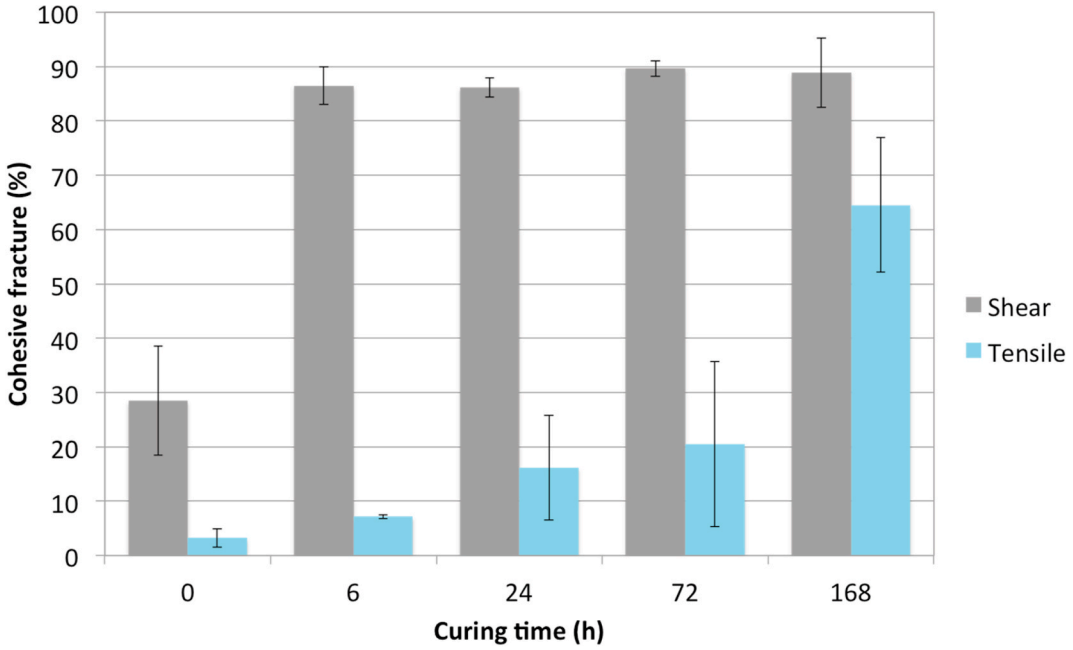

Fig. 11. Percentage of cohesive fracture of shear and tensile joints for different curing times.

Representative Stress-Elongation curves of the tensile and shear tests of the joints with surface treatment T_3 are shown in Fig. 9. It can be seen in this figure that when the joint is subjected to shear stress, the PSA shows a greater YS and UTS values than when subjected to tensile stress. Thus, both YS and UTS values practically coincide in shear test, as very low plastic region appear. This means that this PSA presents relatively high UTS values, but low ductility and toughness values under shear stress. In the case of the tensile tests, the adhesive develops considerable deformation and toughness after the yield strength, showing a plateau at the plastic region, but limited UTS values. This tensile curve shape is characteristic of elastomer materials, as they absorb higher amounts of energy while stretching, showing high toughness [36,39–42].

The overall results of this section show that both roughness and surface treatments have important effects on the PSA mechanical performance. Low roughness surfaces and the application of adhesion promoter are important considerations to improve the bonding ability of the PSA.

3.3. *Influence of curing time*

The influence of the different curing parameters on the PSA tensile and shear mechanical behaviour is covered in sections 3.3 to 3.5. In these following sections, T_3 surface treatment was applied to all joints. Some additional parameters are taken into account, such as the percentage of cohesive rupture, the toughness and ductility of the joints.

Fig. 10 depicts the UTS values, for both tensile and shear tests,

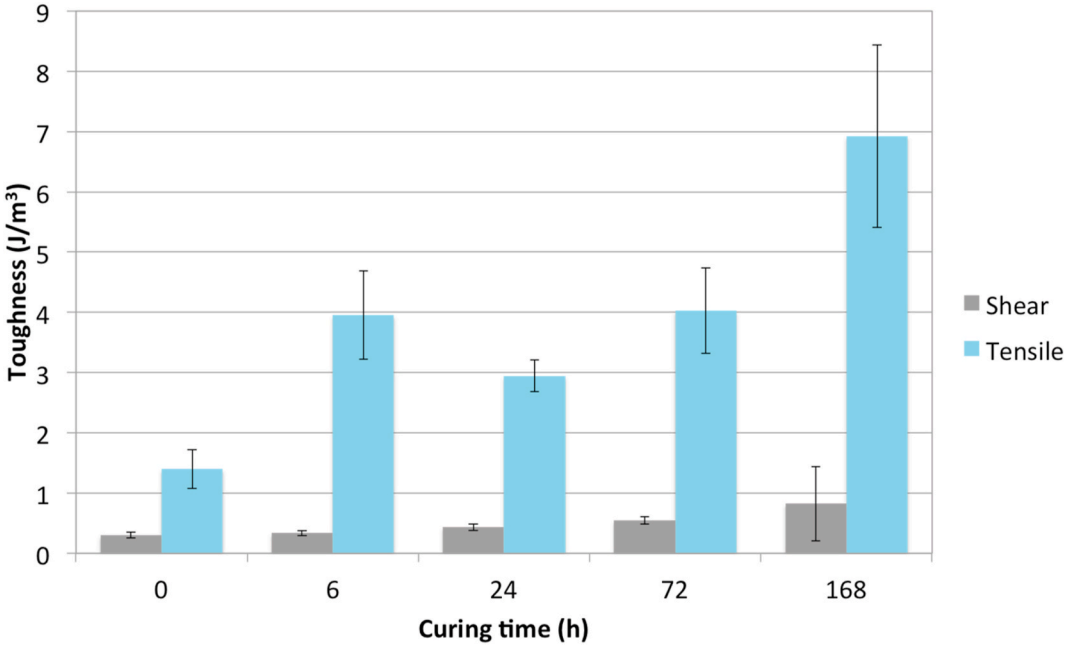

Fig. 12. Toughness measured for shear and tensile tests of PSA as a function of the curing time.

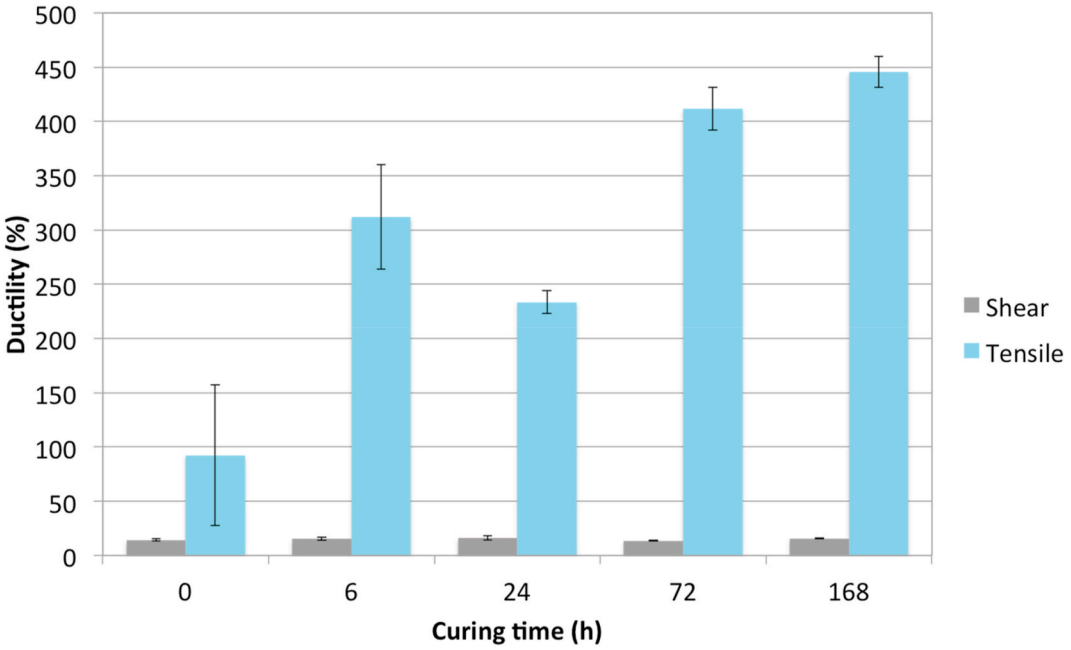

Fig. 13. PSA elongation for different mature times studied.

obtained when the curing time of the PSA was modified. In these tests, the other variables were kept constant: 15 N/cm^2 of compression force during 1 min. Similar and relatively high values were measured for all curing time values tested. It is especially interesting to note that even though at 0 h of curing time (testing just after joining the samples), the PSA works with high performance. This represents an advantage over other adhesives because this kind of adhesives reach a high percentage of their maximum resistance from the first moment of application.

Fig. 11 reports the percentage values of cohesive fracture of shear and tensile joints for different curing times. It can be seen that the tested joint after being assembled has a practically adhesive break. However, with a curing time of 6 h, a practically cohesive fracture is observed at shear tests. These results indicate that the adhesive begins to work at almost maximum shear performance just after 6 h of curing time. Therefore, a reduction of curing time from the 72 h recommended by the manufacturer to just 6 h, does not seem to generate a significant loss of shear resistance in this PSA. Concerning the tensile behaviour of the PSA, it is noticeable that the percentage of cohesive fracture increases linearly with the curing time, reaching its maximum value at 168 h. These results indicate that longer curing times are recommended if the PSA is required to work at tensile stress.

Fig. 12 shows the toughness of the adhesive for the different curing times studied. For shear tests, similar and low values of static toughness are observed, with a little increase for a curing time of 168 h. The joints subjected to tensile stress presented much higher toughness values that the shear joints, as expected from the shape of the representative stress-

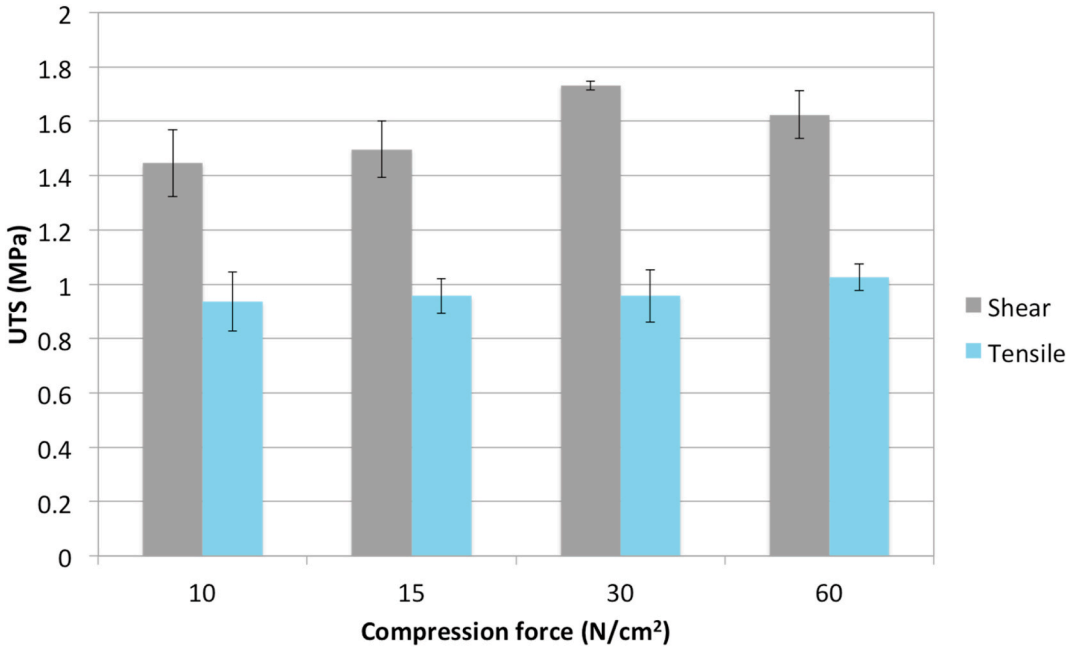

Fig. 14. Variation of the UTS values of shear and tensile tests as a function of the compression force applied.

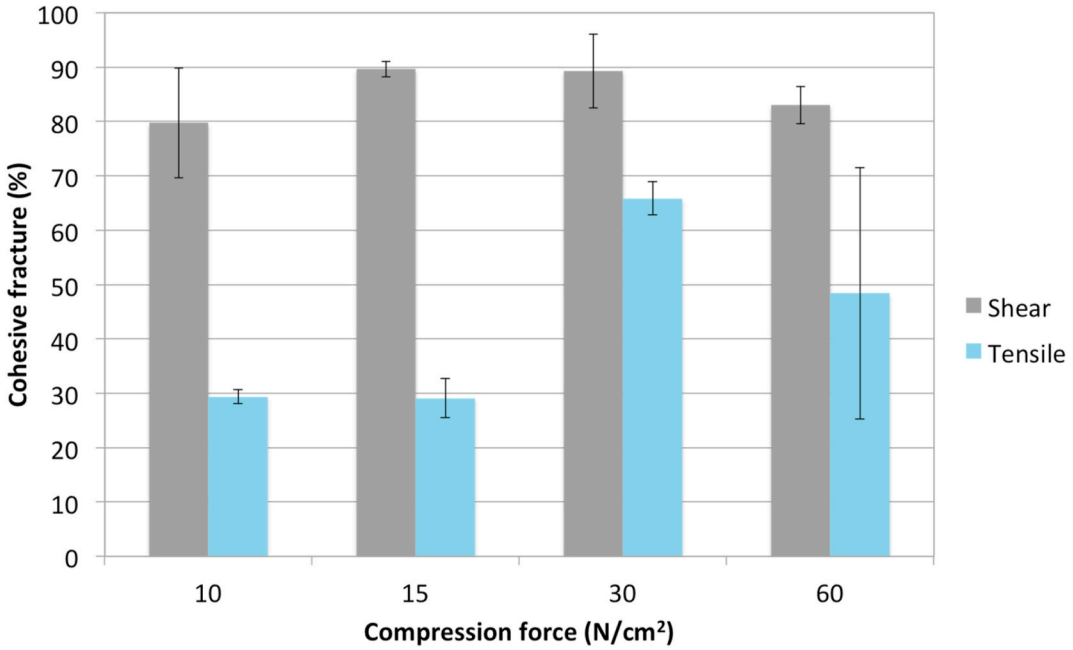

Fig. 15. Percentage of cohesive fracture of tensile and shear tests as a function of the compression force applied.

elongation curves of the tests (Fig. 9). This tensile joints also presented the maximum toughness values for the highest curing time tested (168 h). These data indicate that for tensile stresses, the curing time has a strong influence of UTS and toughness of the joints, being recommended to work with relatively high values of curing times.

Fig. 13 shows the ductility values of the PSA, extracted from the shear and tensile tests, for the different curing times. For shear tests, the curing time does not influence much the ductility of the PSA, as considerable low values (10–15%) of plastic deformation at fracture are always measured. However, when the PSA is subjected to tensile stress, noticeable high plastic deformation are measured (always higher than 80%), increasing this ductility with the curing time. Thus, the best ductility result, close to 450%, is observed for 168 h of curing time.

Therefore, according to these before discussed results, the PSA always presents higher UTS values at shear than at tensile stress, although the ductility and toughness are clearly better at tensile configuration. The influence of the curing time has been observed to be different for shear and tensile stresses. Thus, at shear configuration, the maximum UTS value and reasonable high percentage of cohesive fracture appear at only 6 h of curing time. Meanwhile, at tensile stress, 168 h of curing time are observed to be needed to obtain high values of cohesive fracture.

3.4. *Influence of compression force*

Fig. 14 shows the UTS results of tensile and shear tests when the applied compression force was modified. It is important to consider that

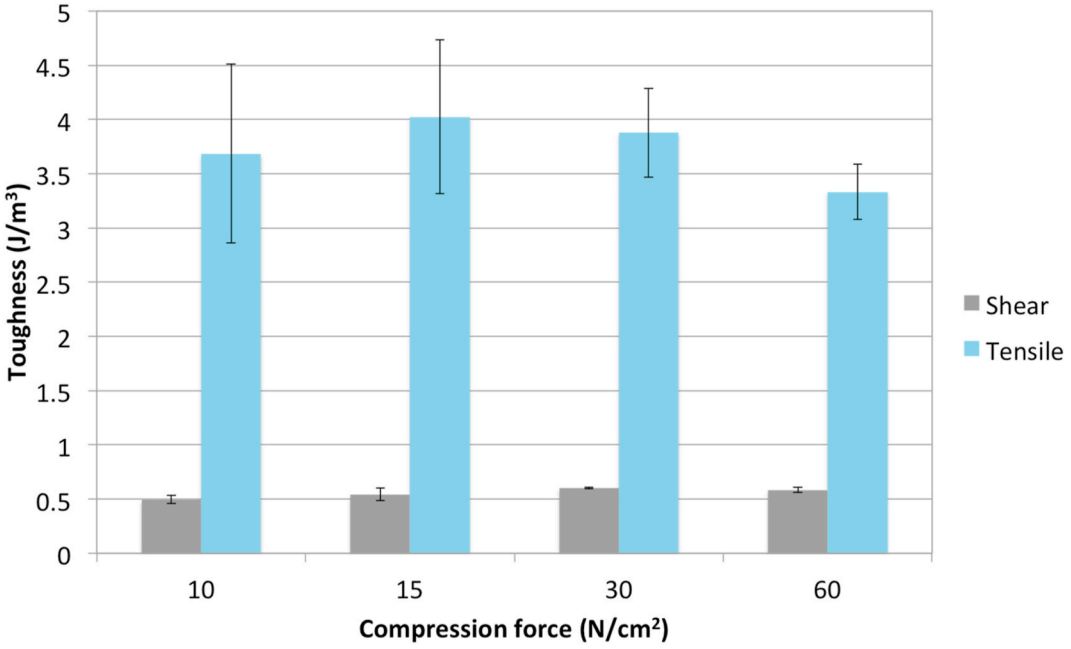

Fig. 16. Effect of the compression force on the toughness of the PSA.

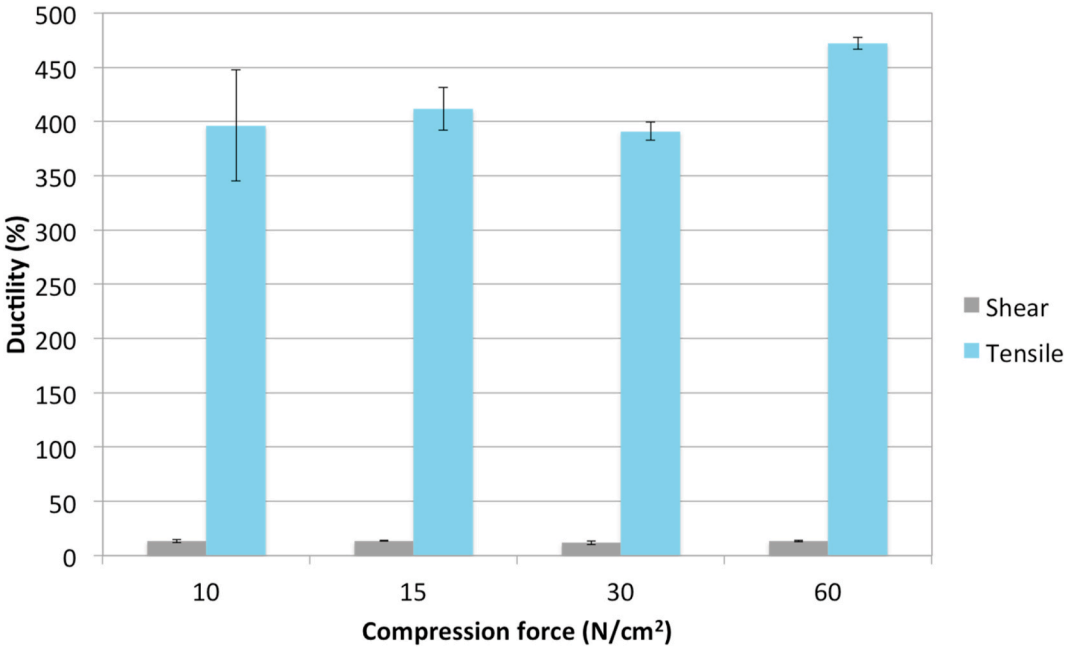

Fig. 17. Ductility for the tensile and shear tests, in function of the compression force applied to the PSA.

compression force values are referred to the applied force per cm^2 of PSA. This figure shows a slight increase in shear strength when 30 N/cm^2 is applied. However, this improvement is not seen in the tensile tests, where the results are similar regardless of the applied compression force, indicating that this variable does not significantly affect the tensile strength.

Fig. 15 shows the percentage of cohesive fracture measured for both shear and tensile tests, when the applied compression force was modified. In shear configuration, the results are quite satisfactory, as higher values than 80% are achieved for all tests. Although slightly higher UTS results were observed when 15 or 30 N/cm^2 was applied, similar values were measured in all cases. In tensile tests, all values were lower than 70%, although the percentage of cohesive fracture rises as the compression force increases. Thus, when the compression force was increased from 10 to 30 N/cm^2 the percentage of cohesive fracture measured was enhanced from 28% to 65%.

In view of the results obtained in Figs. 14 and 15, the compression force of 30 N/cm^2 seems to be the most appropriate for the PSA work in both configurations. Fig. 16 shows the toughness results obtained for both shear and tensile tests after applying different compression forces. When the PSA was subjected to shear stress, the toughness ranged from 0.5 to 0.6 J/m^3, while for tensile tests, the toughness reached between 3.3 and 4.0 J/m^3.

Fig. 17 depicts the ductility of the tested joints. As expected, similar low plastic deformation values were measured for all shear tests. Meanwhile, for the tensile tests, all ductility values were higher than

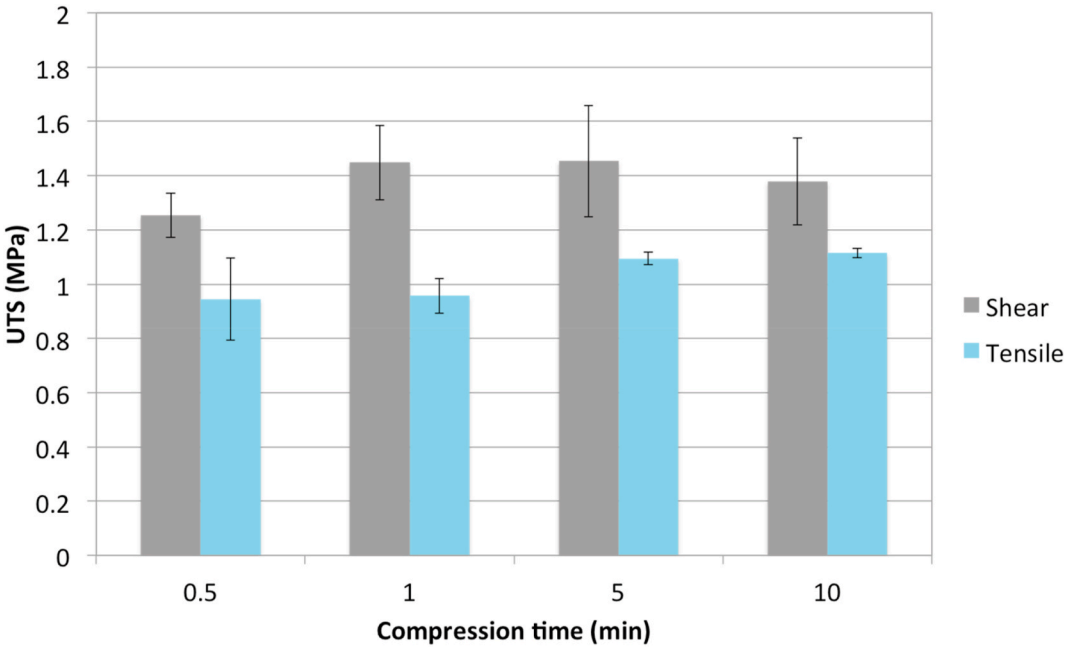

Fig. 18. Variation of the UTS values of shear and tensile tests as a function of the compression time.

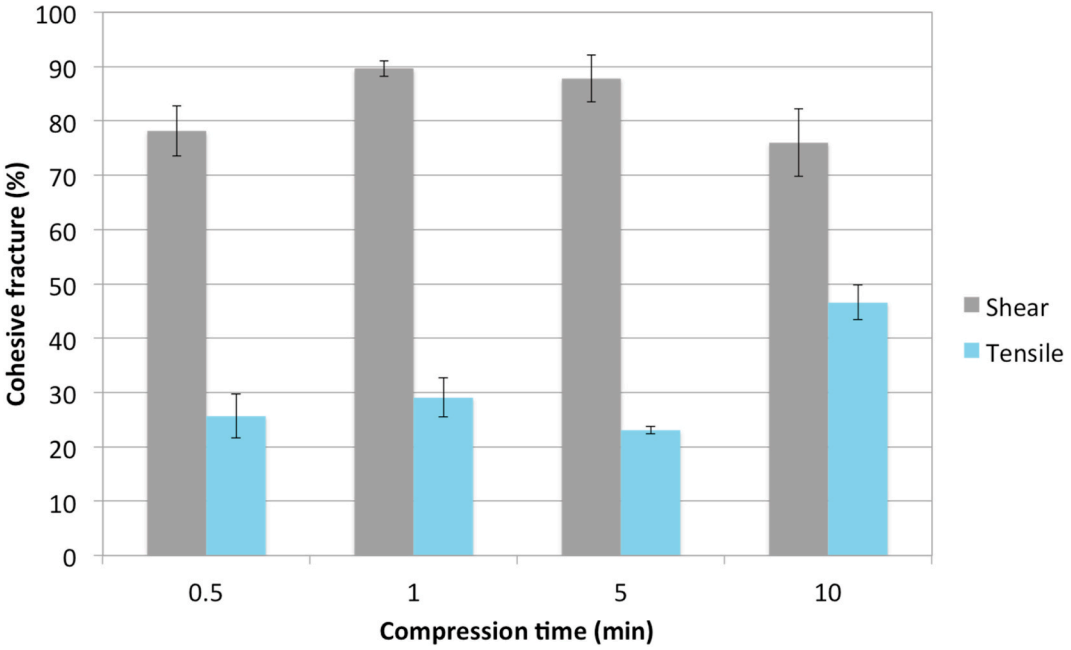

Fig. 19. Percentage of cohesive fracture of tensile and shear tests as a function of the compression time.

350%, being 480% the highest result, obtained when a compression force of 60 N/cm^2 was applied.

In short, taking into account the overall results of this section, it seems that 30 N/cm^2 is an adequate compression force for both tensile and shear configurations. This condition leads to a good combination of high values of UTS, percentage of cohesive adhesion, ductility, and toughness.

3.5. Influence of compression time

Fig. 18 displays the UTS results of both shear and tensile tests in function of the compression time. As in previous sections, UTS of shear tests were higher than those of tensile tests. The figure shows that an increase in compression time does not lead to a significant improvement in joint strength. It is observed that for the shortest compression time studied, 0.5 min, the joints already achieves an acceptable mechanical performance, comparable to the rest of the compression times studied. For tensile configuration, slightly higher UTS values were measured above 5 min of compression, reaching UTS values above 1 MPa.

Fig. 19 shows the percentage of cohesive fracture of the mechanical tests. Figs. 18 and 19 indicate that for shear configuration, 1 min of compression time is enough to achieve maximum PSA adhesion to the painted surface. For tensile configuration, an increase in compression time leads to a slight improvement in PSA adhesion to surfaces, observable at the higher values of both UTS and percentage of cohesive fracture.

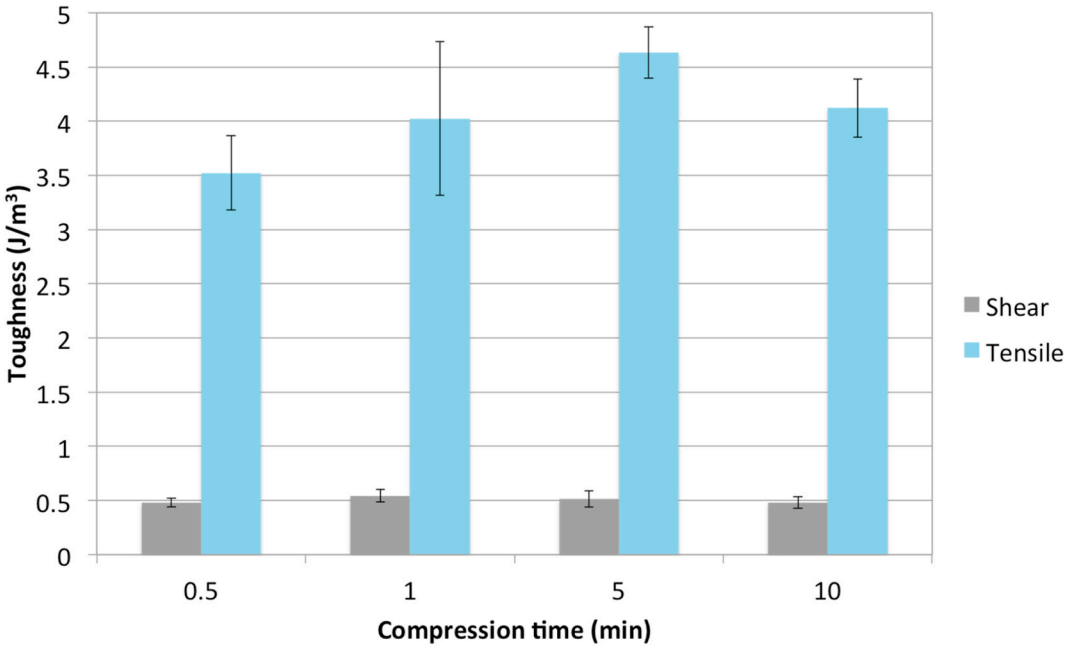

Fig. 20. Effect of compression time on the PSA toughness.

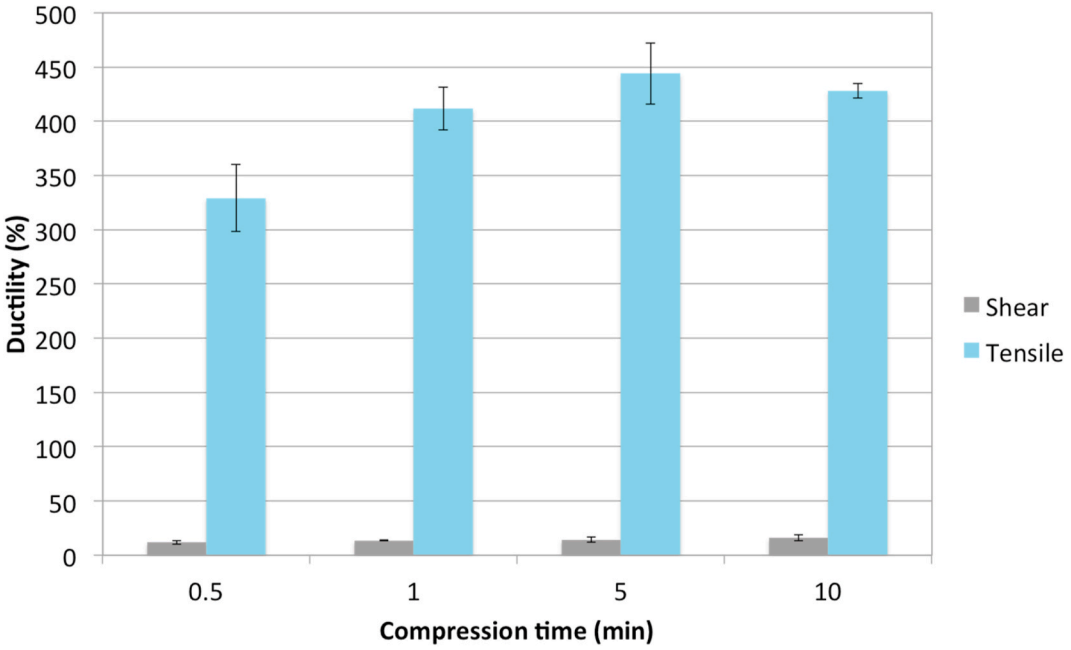

Fig. 21. Effect of compression time on the PSA ductility.

Fig. 20 shows the toughness results obtained from the shear and tensile tests, in function of the different compression times studied. When the PSA is subjected to shear stress, the compression time is not influential in the toughness developed by the adhesive. For tensile tests, an improvement in toughness is observed when a compression time of 5 min is applied. These toughness results agree with those of UTS (Fig. 18), improving both properties when high values of compression times are employed.

Fig. 21 shows the ductility of the PSA after mechanical tests. As expected, in the shear tests, the plastic deformation is again low and practically the same for the different compression times studied. In the case of tensile tests, and as reflected in the toughness graph, the highest elongation is obtained for a compression time of 5 min.

After analysing the influence of the compression time, the overall results show that for shear configuration, 1 min of compression time is enough to achieve maximum PSA adhesion, while for tensile configuration joints, 5 min are required to obtain reasonable mechanical behaviour.

4. Conclusions

In the present work, the mechanical behaviour of a high performance Pressure Sensitive Adhesive has been studied when applied to steel samples coated with an epoxy coating scheme commonly used by the naval industry. As far as the authors are concerned, it is the first research study analysing the influence of experimental application variables of

this PSA-coated system on the mechanical behaviour of joints. Standard shear and tensile tests have allowed us to obtain the values of UTS, percentage of cohesive fracture, ductility and toughness of different joints configurations. In general terms, the PSA shows higher UTS and percentage of cohesive fracture in shear configuration, while higher ductility and toughness in tensile configuration.

The surface roughness, the application of surface treatments, and the curing conditions have been proved to have important effects on the PSA mechanical performance. Low roughness and the application of adhesion promoter to activate the paint surface have been checked to be positive to improve the bonding behaviour of the PSA. The curing time has been observed to affect differently at shear and tensile tests. Thus, while reasonable good mechanical performance is measured at only 6 h of curing time at shear configuration, 168 h of curing time are recommended for tensile tests. The compression force is also checked to be important. 30 N/cm^2 seems a suitable value for both tensile and shear configurations. Concerning the compression time, 1 min is enough to achieve reasonable mechanical behaviour for shear configuration, while 5 min are required for tensile configuration.

Regardless of these different experimental application conditions leading to the best mechanical performance at shear and tensile configuration, in general terms, the mechanical behaviour of the joints is similar in the range of studied values of curing time (0–168 h), compression force (10–60 N) and compression time (0.5–10 min). These results are of great industrial interest, as they show that this PSA maintains high performance with different experimental curing conditions.

Author statement

M. Ortega-Iguña: Investigation, Visualization, Methodology, Formal analysis, Software, Validation, Writing - Original Draft. **M. Chludzinski:** Conceptualization, Methodology, Data Curation, Validation, Writing - Original Draft. **C. Churiaque:** Investigation, Visualization, Resources, Validation. **R.E. dos Santos:** Investigation, Visualization, Validation. **M. Porrúa-Lara:** Supervision. **F. Abad-Fraga:** Supervision. **J.M. Sánchez-Amaya:** Conceptualization, Resources, Project administration, Supervision, Writing - Review & Editing.

Funding

This research is part of Ms. Marta Ortega's PhD, industrial doctoral thesis financed by Vicerrectorado de Política Científica y Económica of the University of Cádiz (Contract reference TDI-18-18).

Declaration of competing interest

The authors declare that they have no known competing financial interests or personal relationships that could have appeared to influence the work reported in this paper.

Acknowledgments

The present study is part of Ms. Marta Ortega's PhD. Authors would like to thank to the Vicerrectorado de Política Científica y Económica of the University of Cádiz for the financial support of her industrial doctoral thesis. Likewise, Navantia S.A. S.M.E. is acknowledged for the technical assistance and guidance related to the materials and components of greatest naval interest. TESA S.A. is also thanked for providing the adhesive tapes and cleaning products used in this work. The support from Department of Mechanical Engineering and Industrial Design (TEP 027 research group) of the University of Cádiz is also gratefully acknowledged.

References

[1] G. Gierenz, W. Karmann, Adhesives and adhesive tapes. Adhesives and adhesive Tapes, 2001, https://doi.org/10.1002/9783527612802.
[2] R. Ciardiello, Mechanical characterization and separation tests of a thermoplastic reinforced adhesive used for automotive applications, Procedia Struct. Integr. 24 (2019) 155–166, https://doi.org/10.1016/j.prostr.2020.02.014.
[3] M.D. Banea, L.F.M. Da Silva, Adhesively bonded joints in composite materials: an overview. Proceedings of the Institution of Mechanical Engineers, Part L, J. Mater.: Des. Appl. 223 (1) (2009) 1–18, https://doi.org/10.1243/14644207JMDA219.
[4] M.D. Banea, M. Rosioara, R.J.C. Carbas, L.F.M. da Silva, Multi-material adhesive joints for automotive industry, Compos. B Eng. 151 (June) (2018) 71–77, https://doi.org/10.1016/j.compositesb.2018.06.009.
[5] A. Biel, K.S. Alfredsson, T. Carlberger, Adhesive Tapes; cohesive laws for a soft layer, Procedia Mater. Sci. 3 (2014) 1389–1393, https://doi.org/10.1016/j.mspro.2014.06.224.
[6] Donatas Satas, Handbook of Pressure Sensitive Adhesive Technology, second ed., Van Nostrand Reinhold, New York, 1989, 0442280262-9780442280260.
[7] S. Lee, J. Back, G. Shim, S. Jang, H. Kim, International Journal of Adhesion and Adhesives Adhesion performance and optical properties of optically pressure-sensitive adhesives including an isosorbide, Int. J. Adhesion Adhes. (November) (2019) 102503, https://doi.org/10.1016/j.ijadhadh.2019.102503.
[8] Z. Czech, Solvent-based pressure-sensitive adhesives for removable products, Int. J. Adhesion Adhes. 26 (6) (2006) 414–418, https://doi.org/10.1016/j.ijadhadh.2005.06.009.
[9] J.H. Lee, T.H. Lee, K.S. Shim, J.W. Park, H.J. Kim, Y. Kim, S. Jung, Effect of crosslinking density on adhesion performance and flexibility properties of acrylic pressure sensitive adhesives for flexible display applications, Int. J. Adhesion Adhes. 74 (January) (2017) 137–143, https://doi.org/10.1016/j.ijadhadh.2017.01.005.
[10] S. Kim, S.W. Lee, D.H. Lim, J.W. Park, C.H. Park, H.J. Kim, Fabrication of optically clear acrylic pressure-sensitive adhesive by photo-polymerization: UV-curing behavior, adhesion performance, and optical properties, J. Adhes. Sci. Technol. 27 (20) (2013) 2177–2190, https://doi.org/10.1080/01694243.2013.763480.
[11] N. Ishikawa, M. Furutani, K. Arimitsu, Pressure-sensitive adhesive utilizing molecular interactions between thymine and adenine, J. Polym. Sci. Polym. Chem. 54 (10) (2016) 1332–1338, https://doi.org/10.1002/pola.27977.
[12] Z. Czech, Crosslinking of pressure sensitive adhesive based on water-borne acrylate, Polym. Int. 52 (3) (2003) 347–357, https://doi.org/10.1002/pi.1151.
[13] Z. Czech, A. Butwin, U. Gluch, J. Kabatc, Influence of selected photoinitiators on important properties of photoreactive acrylic pressure-sensitive adhesives, J. Appl. Polym. 123 (2012) 118–123.
[14] Z. Yang, H. Peng, W. Wang, T. Liu, Crystallization behavior of poly (ε-caprolactone)/layered double hydroxide nanocomposites, J. Appl. Polym. Sci. 116 (5) (2010) 2658–2667, https://doi.org/10.1002/app.
[15] I.J. Chin, T. Thurn-Albrecht, H.C. Kim, T.P. Russell, J. Wang, On exfoliation of montmorillonite in epoxy, Polymer 42 (13) (2001) 5947–5952, https://doi.org/10.1016/S0032-3861(00)00898-3.
[16] A.S. Zerda, A.J. Lesser, Intercalated clay nanocomposites: morphology, mechanics, and fracture behavior, J. Polym. Sci. B Polym. Phys. 39 (11) (2001) 1137–1146, https://doi.org/10.1002/polb.1090.
[17] J.J. Luo, I.M. Daniel, Characterization and modeling of mechanical behavior of polymer/clay nanocomposites, Compos. Sci. Technol. 63 (11) (2003) 1607–1616, https://doi.org/10.1016/S0266-3538(03)00060-5.
[18] S. Hayashida, T. Sugaya, S. Kuramoto, C. Sato, International Journal of Adhesion & Adhesives. Impact Strength of Joints Bonded with High-Strength Pressure-Sensitive Adhesive, vol. 56, 2015, pp. 61–72.
[19] M. Horgnies, E. Darque-Ceretti, E. Felder, Relationship between the fracture energy and the mechanical behaviour of pressure-sensitive adhesives, Int. J. Adhesion Adhes. 27 (8) (2007) 661–668, https://doi.org/10.1016/j.ijadhadh.2006.12.002.
[20] A.V. Kostyuk, V.Y. Ignatenko, S.V. Antonov, S.O. Ilyin, International Journal of Adhesion and Adhesives. Effect of Surface Contamination on the Durability and Strength of Stainless Steel – Polyisobutylene Pressure-Sensitive Adhesive Bonds, 2019.
[21] J.J.M. Machado, P.D.P. Nunes, E.A.S. Marques, F.M. Lucas, Adhesive Joints Using Aluminium and CFRP Substrates Tested at Low and High Temperatures under Quasi-Static and Impact Conditions for the Automotive Industry, 2018.
[22] L. Sa, R. Balart, R. Sanchis, O. Fenollar, D. Garcı, International Journal of Adhesion & Adhesives Improved Adhesion of LDPE Films to Polyolefin Foams for Automotive Industry Using Low-Pressure Plasma, vol. 28, 2008, pp. 445–451, https://doi.org/10.1016/j.ijadhadh.2008.04.002.
[23] N. Kalapat, T. Amornsakchai, Surface modification of biaxially oriented polypropylene (BOPP) film using acrylic acid-corona treatment : Part I . Properties and characterization of treated films, Surf. Coating. Technol. 207 (2012) 594–601, https://doi.org/10.1016/j.surfcoat.2012.07.081.
[24] S. Park, S. Song, J. Shin, J. Rhee, Effect of Surface Oxyfluorination on the Dyeability of Polyethylene Film, 283, 2005, pp. 190–195, https://doi.org/10.1016/j.jcis.2004.02.094.
[25] Y. Wang, J. Long, Y. Bai, C. Zhang, B. Cheng, L. Shao, S. Qi, Preparation and characterization of fluorinated acrylic pressure sensitive adhesives for low surface energy substrates, J. Fluor. Chem. 180 (2015) 103–109, https://doi.org/10.1016/j.jfluchem.2015.09.007.
[26] C. Gay, L. Leibler, Theory of tackiness, Phys. Rev. Lett. 82 (5) (1999) 936–939, https://doi.org/10.1103/PhysRevLett.82.936.
[27] I. Benedek, Pressure-Sensitive Adhesives and Applications, second ed., Pstc, 2004. Revised and Expanded.

[28] A. Chiche, P. Pareige, C. Creton, Role of surface roughness in controlling the adhesion of a soft adhesive on a hard surface, Comptes Rendus Acad. Sci. - Ser. IV Phys., Astrophys. 1 (9) (2000) 1197–1204, https://doi.org/10.1016/S1296-2147(00)01133-1.

[29] V. Daniloska, P. Carretero, R. Tomovska, J.M. Asua, High performance pressure sensitive adhesives by miniemulsion photopolymerization in a continuous tubular reactor, Polymer 55 (20) (2014) 5050–5056, https://doi.org/10.1016/j.polymer.2014.08.038.

[30] M. Iseki, Y. Suzuki, H. Tachi, A. Matsumoto, Design of a high-performance dismantlable adhesion system using pressure-sensitive adhesive copolymers of 2-hydroxyethyl acrylate protected with tert-butoxycarbonyl group in the presence of cross-linker and lewis acid, ACS Omega 3 (11) (2018) 16357–16368, https://doi.org/10.1021/acsomega.8b02371.

[31] S.S. Baek, S.H. Jang, S.H. Hwang, Construction and adhesion performance of biomass tetrahydro-geraniol-based sustainable/transparent pressure sensitive adhesives, J. Ind. Eng. Chem. 53 (2017) 429–434, https://doi.org/10.1016/j.jiec.2017.05.017.

[32] M. Bartkowiak, Z. Czech, K. Mozelewska, J. Kabatc, Comparison between Thermal Crosslinkers Based on Melamine-Formaldehyde and Benzoguanamine Resin and Their Influence on Main Performance of Acrylic Pressure-Sensitive Adhesives as Tack, Peel Adhesion, Shear Strength and pot-life.Pdf, 89, 2020 (February).

[33] I. Erukhimovich, M.O. de la Cruz, Phase Equilibria and Charge Fractionation in Polydisperse Polyelectrolyte Solutions, 2004, pp. 1237–1252, https://doi.org/10.1002/polb.

[34] I.K. Mohammed, M.N. Charalambides, A.J. Kinloch, Modeling the effect of rate and geometry on peeling and tack of pressure-sensitive adhesives, J. Non-Newtonian Fluid Mech. 233 (2016) 85–94, https://doi.org/10.1016/j.jnnfm.2016.01.016.

[35] S. Sun, M. Li, A. Liu, A review on mechanical properties of pressure sensitive adhesives, Int. J. Adhesion Adhes. 41 (2013) 98–106, https://doi.org/10.1016/j.ijadhadh.2012.10.011.

[36] J.H. Lee, M.H. Myung, M.J. Baek, H.S. Kim, D.W. Lee, Effects of monomer functionality on physical properties of 2-ethylhexyl acrylate based stretchable pressure sensitive adhesives, Polym. Test. 76 (2019) 305–311, https://doi.org/10.1016/j.polymertesting.2019.03.033. February.

[37] Y. Wang, J. Long, Y. Bai, C. Zhang, B. Cheng, L. Shao, S. Qi, Preparation and characterization of fluorinated acrylic pressure sensitive adhesives for low surface energy substrates, J. Fluor. Chem. 180 (2015) 103–109, https://doi.org/10.1016/j.jfluchem.2015.09.007.

[38] A. Kowalski, Z. Czech, The effects of substrate surface properties on tack performance of acrylic Pressure-Sensitive Adhesives (PSAs), Int. J. Adhesion Adhes. 60 (2015) 9–15, https://doi.org/10.1016/j.ijadhadh.2015.03.004.

[39] A. Zosel, The effect of fibrilation on the tack of pressure sensitive adhesives, Int. J. Adhesion Adhes. 18 (4) (1998) 265–271, https://doi.org/10.1016/S0143-7496(98)80060-2.

[40] A. Chiche, J. Dollhofer, C. Creton, Cavity growth in soft adhesives, Eur. Phys. J. E 17 (4) (2005) 389–401, https://doi.org/10.1140/epje/i2004-10148-3.

[41] T. Yamaguchi, H. Morita, M. Doi, Modeling on debonding dynamics of pressure-sensitive adhesives, Eur. Phys. J. E 20 (1) (2006) 7–17, https://doi.org/10.1140/epje/i2005-10078-6.

[42] F. Tanguy, M. Nicoli, A. Lindner, C. Creton, Quantitative analysis of the debonding structure of soft adhesives, Eur. Phys. J. E 37 (1) (2014) 1–11, https://doi.org/10.1140/epje/i2014-14003-8.